

# The effect of boro-tempering heat treatment on the properties of ductile cast iron

Y. Yalçın\*, A. M. Yazıcı

*Afyonkarahisar Kocatepe University, Technical Education Faculty, Department of Metal Education, Afyonkarahisar 03200, Turkey*

Received 4 July 2006, received in revised form 17 October 2006, accepted 17 October 2006

## Abstract

In this study, the effect of boro-tempering heat treatment on the microhardness, impact toughness and microstructure of ductile cast iron has been investigated. Boro-tempering is a heat treatment combining traditional boronizing and austempering processes. Microstructural characterization of the heat treated ductile cast iron was carried out by using optical microscopy, scanning electron microscopy, and X-ray diffraction analysis. The thickness of the boride layer and the hardness change from surface to matrix were measured by the Vickers indentation technique. X-ray diffraction analysis showed that the boride layer formed on the surface of boro-tempered ductile cast iron consisted of dominantly  $\text{Fe}_2\text{B}$  and a small amount of  $\text{FeB}$  phases. The thickness increased with the boronizing time but was not affected by the cooling rate after the boronizing treatment. It was observed that boro-tempered ductile cast iron has a higher surface hardness and higher impact toughness than that of standard ductile cast iron; it also has a higher surface hardness than that of austempered ductile iron.

**Key words:** iron alloys, mechanical properties, microstructure, Scanning Electron Microscopy (SEM), boro-tempering

## 1. Introduction

The term austempered ductile iron (ADI) describes a range of ductile cast irons that are subjected to an austempering heat treatment to produce an essentially ausferritic structure in the materials. Austempering is an isothermal heat treatment process involving two main stages. The first stage (austenitizing) involves the heating of castings within the range 850–950 °C, followed by rapid quenching to a lower temperature within the range 235–450 °C. The second stage involves austempering at this temperature for between 0.5 and 4 hours [1, 2]. Quenching to the austempering temperature must be fast enough to avoid the pearlitic transformation if the maximum attainable toughness and ductility are to be realized. Austempering is performed above the martensite start (Ms) temperatures [3].

ADI can be twice as strong as the standard ductile cast iron at the same level of ductility. Tensile strengths ranging from 800 MPa with more than 10%

elongation to over 1400 MPa with 2–3% elongation can be achieved depending on the heat treatment parameters and chemical composition [4]. The materials have also been shown to exhibit greater impact toughness, fatigue strength and wear resistance. These good properties are directly related to the unique microstructure consisting of acicular, carbide-free ferrite with large amounts of retained austenite [5, 6].

Numerous studies have evaluated the mechanical properties of ADI including tensile strength, fracture toughness, fatigue properties, wear and pitting resistance [7–13]. A wide range of properties of ADI is available based on the selection of heat treatment parameters and therefore the potential for use of this material is very wide. In [14], a number of successful applications for ADI have been summarized and demonstrated that this new family of materials can have both technical and commercial advantages.

On the other hand, the use of hard coatings on the surfaces of various engineering components has dramatically increased in recent years. This trend reflects

\*Corresponding author: tel.: +90 272 228 13 11; fax: +90 272 228 13 19; e-mail address: [yvalcin@aku.edu.tr](mailto:yvalcin@aku.edu.tr)

the ever-increasing need for higher performance materials for use in extreme application conditions. Boronizing is a thermochemical surface treatment process in which boron atoms are diffused into the surface of a workpiece to form borides ( $\text{FeB}$  and  $\text{Fe}_2\text{B}$ ) with the base materials [15]. The borided layer on the outer surface of the material is supported by the diffusion zone, which extends into the materials. Industrial boronizing can be applied to most ferrous materials, such as structural steels, cast steels, Armco iron and sintered iron as well as to non-ferrous metals [16, 17]. Ductile and grey cast irons have also been successfully boronized [18, 19].

Boronizing can be performed in numerous ways, including conventional (i.e. salt bath, paste and pack boriding) and advanced (i.e. plasma based) techniques. Boride layers possess a number of characteristic features with special advantages over conventional case hardened layers. One basic advantage is that boride layers have extremely high hardness values (between 1450 and 5000 HV) with high melting points of the constituent phases [18]. Completely integral with the substrate, boronizing improves resistance to wear and corrosion [20, 21].

Austempering heat treatment provides ductile cast iron with superior properties such as high strength, fracture toughness and fatigue resistance. On the other hand, boronizing heat treatment yields excellent wear resistance, high surface hardness and corrosion resistance. Thus, if austempering is combined with boronizing, it should provide ductile iron with a matrix having a high strength and fracture toughness and a surface having a superior hardness and wear resistance. This novel heat treatment will be called boro-tempering from now on. The main objective of this investigation was to examine the feasibility of this heat treatment, i.e. boronizing (austenitizing) and then quenching into a molten salt bath (tempering).

## 2. Experimental procedures

The chemical composition of the ductile cast iron used in this study is given in Table 1. The microstructure of the ductile cast iron consisted of a pearlitic matrix with ferritic rings of varying thicknesses surrounding the graphite nodules, which had a good nodularity (Fig. 1).

Table 1. The chemical composition (wt.%) of ductile cast iron

C	Si	Mn	P	S	Cr	Cu	Mg	Sn
3.64	2.52	0.38	0.051	0.10	0.084	0.26	0.042	0.013

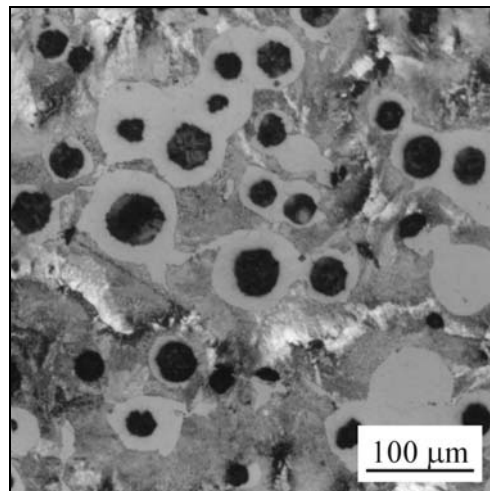


Fig. 1. Optical micrograph of as-cast ductile iron.

Test materials were machined and ground to a rectangular shape with dimensions of  $55 \times 10 \times 10$  mm. Three types of heat treatment were carried out on the specimens, namely boronizing, boro-tempering and austempering. Pack boronizing was selected as the boronizing method since the molten salt bath boronizing technique leaves a salt layer on the specimen, which reduces the austemperability of ductile cast iron. Boronizing was performed in a solid medium containing commercial Ekabor<sup>®</sup>2 powder (the boron donor –  $\text{B}_4\text{C}$ , the activator –  $\text{KBF}_4$  and the filler –  $\text{SiC}$ ) under atmospheric pressure at a temperature of  $900^\circ\text{C}$  for 2 and 5 h. This was followed by cooling in air to room temperature. In boro-tempering, samples were first boronized and then quenched in a molten salt bath at a temperature of  $250^\circ\text{C}$  or  $375^\circ\text{C}$  and held for 1 h. Austempering was carried out by the usual method. It was accomplished by austenitizing at  $900^\circ\text{C}$  for 2 or 5 h in a bed of cast iron chips in an electrically heated furnace, followed by a quench into a salt bath at one of the austempering temperatures,  $250^\circ\text{C}$  or  $375^\circ\text{C}$  and holding for 1 h. All of the heat treatments are summarized in Table 2.

An Olympus optical microscope and a Leo 1430 VP scanning electron microscope were used to examine the microstructure of polished and etched specimens and the fracture surface of the impact tested specimens. Polished samples were etched using 2% Nital. The presence of borides formed in the coating layer was confirmed by means of X-ray diffraction (Shimadzu XRD 6000) using  $\text{CuK}_\alpha$  ( $\lambda = 0.15406$  nm) radiation. The thicknesses of the boride layers formed on samples were measured by an optical micrometer attached to the optical microscope.

The hardness of the boride layers and substrates was measured on the cross-sections using a Shimadzu HMV-2 Vickers indenter with a 100 g load. The un-

Table 2. Heat treating conditions of ductile cast irons

Group of samples	Sample code	Boronizing at 900 °C Time (h)	Austenitizing at 900 °C Time (h)	Tempering temperature (°C)
Boronized and air cooled (BAC)	2BAC	2	–	–
	5BAC	5	–	–
Boro-tempered Ductile Cast Iron (BDI)	225BDI	2	–	250
	525BDI	5	–	250
	237BDI	2	–	375
	537BDI	5	–	375
Austempered Ductile Cast Iron (ADI)	225ADI	–	2	250
	525ADI	–	5	250
	237ADI	–	2	375
	537ADI	–	5	375

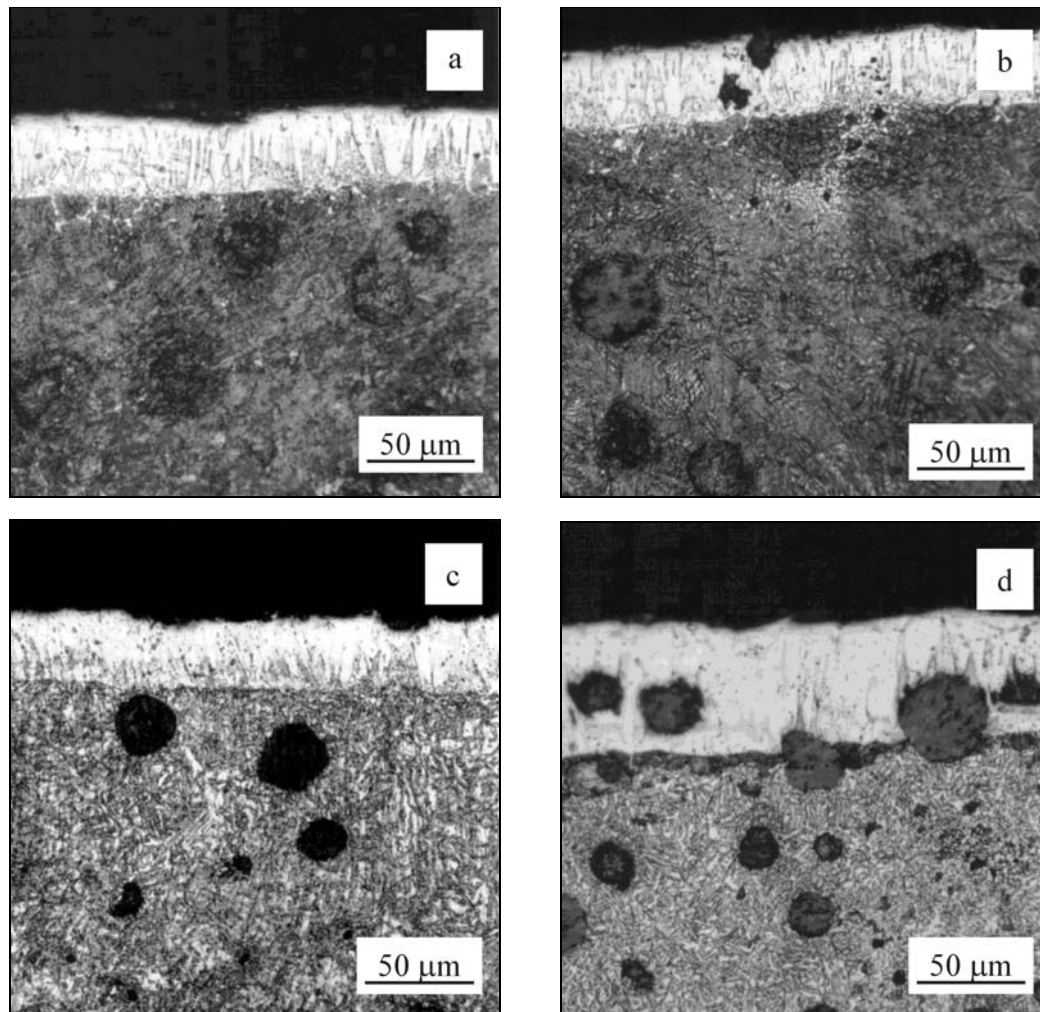


Fig. 2. Optical microscopy images of boronized and boro-tempered ductile cast irons: (a) boronized for 2 h (2BAC), (b) boronized for 2 h and tempered at 250 °C (225BDI), (c) boronized for 2 h and tempered at 375 °C (237BDI), and (d) boronized for 5 h and tempered at 375 °C (537BDI).

notched Charpy impact tests were carried out by a PSd 300/150-1 impact test device. Three tests were

performed under the same conditions to ensure the reproducibility of the impact test data.

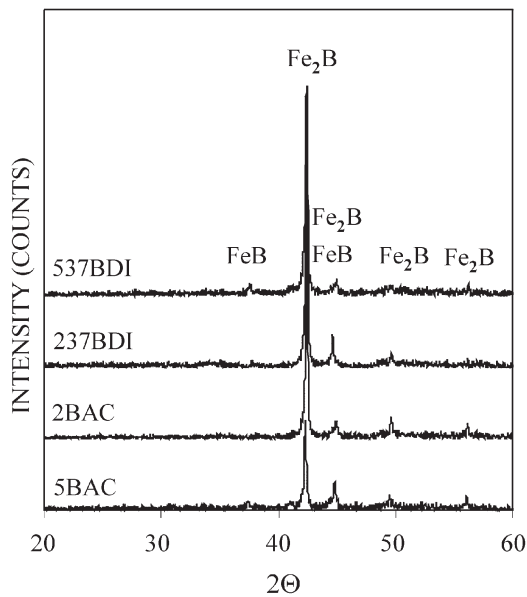


Fig. 3. XRD pattern of boronized and boro-tempered ductile cast iron treated at 900 °C for 2 or 5 h.

### 3. Results and discussion

#### 3.1. Characterization of boride layers

Optical microscopy images of boronized and boro-tempered ductile cast iron are shown in Fig. 2. The boride layer formed on the surface has a tooth-shaped morphology and the layer/matrix interface is seen to be rather smooth. Microstructural examination showed that the thickness of the boride layer depends on the boronizing times, but it is not affected by the cooling conditions. The thicknesses of the boride layers of the boronized and boro-tempered ductile cast irons are  $42 \pm 9$  and  $65 \pm 10$   $\mu\text{m}$  for boronizing times of 2 and 5 h, respectively.

The phases formed on the surface of the boronized and boro-tempered samples at 900 °C for 2 and 5 h were determined by means of XRD analysis as seen in Fig. 3. This shows that boronizing for 2 h gives only  $\text{Fe}_2\text{B}$  peaks while minor  $\text{FeB}$  peaks appear with increased time (5 h).

The isothermal transformation temperature is the major factor affecting the matrix microstructure and mechanical properties of boro-tempered ductile cast iron (BDI) and ADI. While boronized samples have a fine pearlitic microstructure (Fig. 2a), boro-tempered microstructures contain either lower ausferrite (Fig. 2b) or upper ausferrite (Fig. 2c) depending on the transformation temperature. At 250 °C, the growth rate of the ferritic needles is high and as the rate of the carbon diffusion is relatively low, the room temperature matrix is lower ausferrite with a fine, acicular ferrite, a small amount of retained aus-

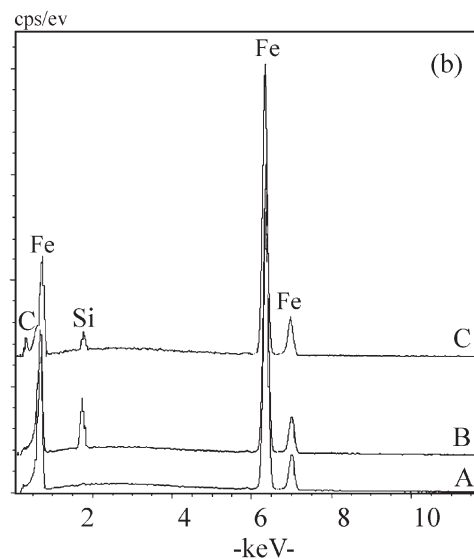
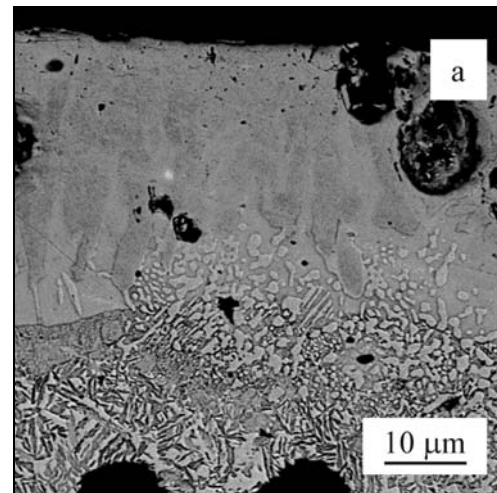


Fig. 4. (a) SEM-BSE image of cross-sectional view of the 537BDI (boronized for 5 h and tempered at 375 °C) sample and (b) EDX spectra of points A, B and C.

tenite and very fine carbides. At higher temperature (375 °C), a different transformation mechanism operates, resulting in the formation of upper ausferrite. Carbon diffusion is more rapid so most of the carbon is able to diffuse out of the ausferritic plates. The structure of upper ausferrite consists of a mixture of relatively coarse, feathery, carbide-free ferrite plates interspersed with high amounts of retained austenite.

Figures 4a and 4b show a SEM-BSE image of the cross-section through the 537BDI sample and EDX analyses taken from three different points. This indicates the formation of a silicon-rich zone between the boride teeth and substrate (point B). Silicon has almost no solubility in iron boride (point A). Therefore, during the boronizing process, silicon atoms diffuse inwards and produce a silicon-rich zone between the boride grains at the front of the boronized layers [22].

Table 3. Hardnesses of surface and matrix and unnotched impact strength of as-cast and heat treated ductile cast iron

Specimen code	Hardness of matrix (HV <sub>0.1</sub> )	Hardness of surface (HV <sub>0.1</sub> )	Unnotched impact toughness (Joule)
As-cast	195	195	26.5
2BAC	285	1602	23.0
5BAC	308	1591	23.0
225BDI	458	1585	26.5
525BDI	380	1595	19.0
237BDI	300	1597	44.0
537BDI	285	1580	79.0
225ADI	475	475	27.0
525ADI	460	460	25.0
237ADI	310	310	120.0
537ADI	295	295	36.0

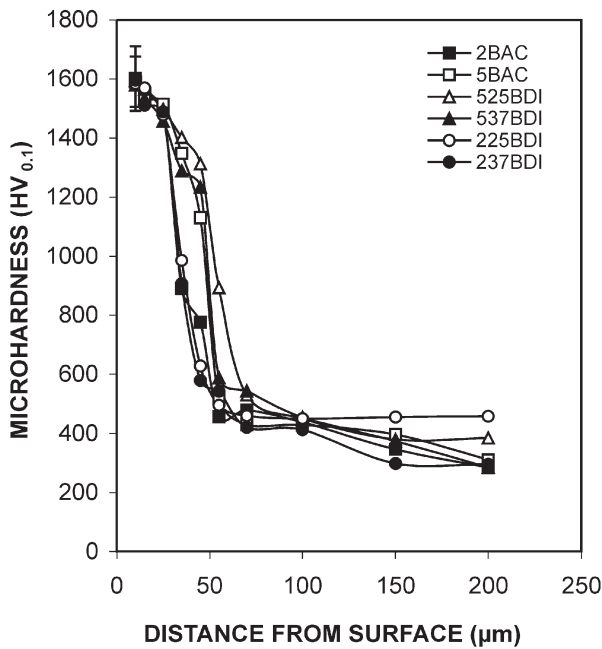


Fig. 5. The variation of microhardness of the boronized and boro-tempered ductile cast irons.

Moreover, carbon atoms do not dissolve significantly in the boride layer and are driven out from the boride layer to the matrix during the boronizing treatment [18, 23, 24].

This shows that there are three distinct regions on the cross-sections of the BDI surfaces. These are: (A) a surface layer dominantly containing Fe<sub>2</sub>B, minor FeB and spheroidal graphite, (B) a silicon-rich zone containing silicon and (C) matrix (lower ausferritic, upper ausferritic or thin pearlitic structure according to type of heat treatment) as shown in SEM-BSE image (Fig. 4).

### 3.2. Hardness and impact tests

Table 3 gives the average values of the surface and

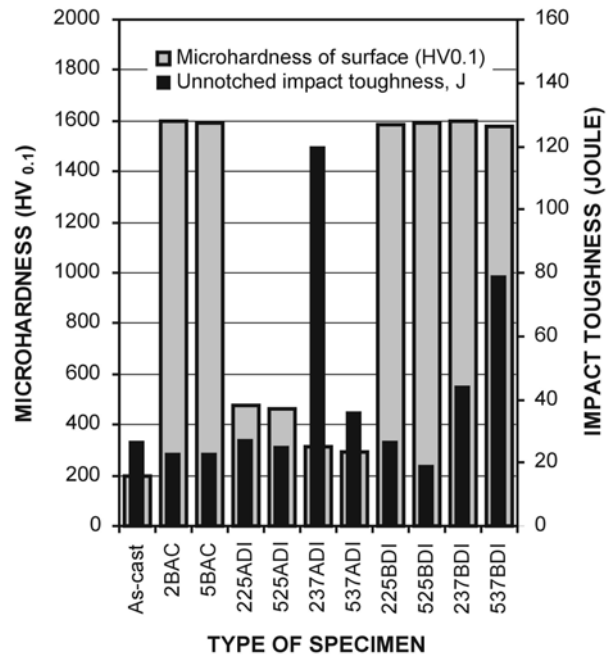


Fig. 6. Unnotched impact toughness and surface hardness values of as-cast and heat treated ductile cast irons.

matrix hardness and unnotched Charpy impact toughness for all samples. The measured values were obtained from different regions of the surface coating. It is considered that the presence of even minor concentration structural defects can slightly influence the hardness values. Actually, the variation range of the hardness values in this study is rather narrow. The maximum hardness values for Fe<sub>2</sub>B and FeB are reported to be 1800–2000 and 1900–2100, respectively [18]. The average hardness values for the boronized and boro-tempered samples in this study ranged from 1580 to 1602 as presented in Table 3. This result, when compared with the reported values by Sinha [18], suggests that the present phase on the surface in the present work should be Fe<sub>2</sub>B, instead of FeB. Indeed, X-ray diffraction patterns of the samples in

Fig. 3 verify the presence of  $\text{Fe}_2\text{B}$  as the major phase on the coating surfaces compared to a very minor existence of  $\text{FeB}$ . The measured hardness values are consistent with both the XRD results and the reported values by Sinha [18].

The changes of microhardness with the distance from the surface for boronized and boro-tempered ductile cast iron are illustrated in Fig. 5. The hardness of the boride layer was found to be three or four times higher than that of lower ausferritic, upper ausferritic and pearlitic matrix structures. As seen in Table 3, 225ADI and 225BDI samples having a lower ausferritic structure have the highest matrix hardness values (475 HV and 458 HV, respectively). The lower amount of retained austenite and the higher amount of needle-like ferrite with carbides cause the higher hardness and lower impact toughness. Increasing isothermal transformation temperature increases the amount of retained austenite and substantially enhances the impact toughness, but reduces the hardness [25].

The values of impact toughness and surface hardness obtained from as-cast and heat treated ductile cast irons are given in Fig. 6. The effect of holding time at high temperatures on the impact toughness of ADI and BDI is different. Maximum impact toughness was obtained by austempering and boro-tempering at  $375^\circ\text{C}$ . However, the maximum impact toughness was obtained in ADI after austenitizing for 2 h, but in BDI after boronizing for 5 h. For either ADI or BDI samples, isothermal transformation at  $250^\circ\text{C}$  gives notably lower impact toughness values. As seen in Fig. 6, the optimum combination of hardness and toughness was obtained by boronizing at  $900^\circ\text{C}$  for 5 h, followed by holding at  $375^\circ\text{C}$  for 1 h which gives an upper ausferritic matrix structure coated by a boride layer. The results show that boro-tempering produces higher impact toughness and higher surface hardness when compared to boronizing and austempering treatments, respectively.

Figure 7 shows SEM images of the fracture surfaces

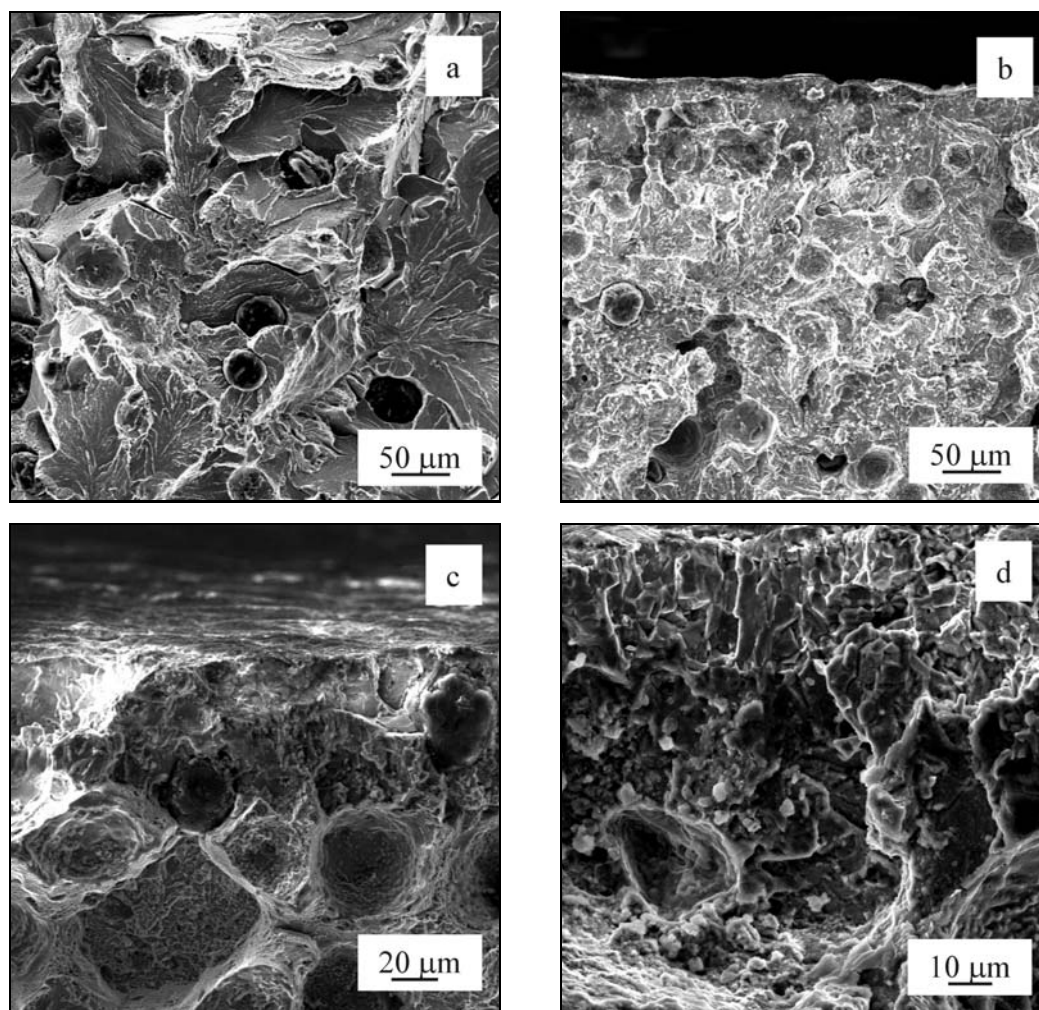


Fig. 7. SEM fracture appearances of (a) as-cast ductile iron, (b) boronized for 5 h (5BAC), (c) boronized for 2 h and tempered at  $250^\circ\text{C}$  (225BDI), (d) boronized for 2 h and tempered at  $375^\circ\text{C}$  (237BDI) after impact loading.

of as-cast ductile iron, boronized ductile cast iron and BDI after impact loading. As seen in Fig. 7a, the as-cast ductile iron fractured by cleavage with no evidence of significant localized plasticity. This cast iron had a pearlitic matrix with ferritic rings of varying thickness surrounding the graphite nodules and exhibited predominantly brittle fracture with river patterns in the pearlitic areas. The fracture appearance of the specimen 5BAC boronized for 5 h and then cooled in air is shown in Fig. 7b. This sample has a pearlitic microstructure and its fracture appearance is different from that of the as-cast ductile iron. It can be clearly seen that the boronized sample has a finer microstructure than the as-cast sample.

Figures 7c and 7d show the fracture surfaces for specimens 225BDI and 237BDI boronized and boro-tempered for 2 h at 250 °C and at 375 °C, respectively. The first one has less retained austenite, compared to upper ausferrite due to the lower tempering temperature and gives lower impact toughness and less dimpled rupture. The fracture surfaces of the coating layers differ from the core as can be seen in Figs. 7c and 7d. Especially it is clearly seen in Fig. 7d that the coating layer fractured surface has a columnar-like morphology unlike the round shaped feature of the core. A high boro-tempering temperature, 375 °C, produces considerably localized plasticity and dimpled rupture between graphite nodules. This may be related to the presence of more retained austenite [25].

#### 4. Conclusions

From this study, the following conclusions can be drawn:

1. Boro-tempering heat treatment was successfully applied to ductile cast iron.
2. The boride layer formed on the surface of the boronized and boro-tempered ductile cast iron consisted mainly of Fe<sub>2</sub>B and a small amount of FeB. The layers on both the boronized and the boro-tempered samples were 42 ± 9 and 65 ± 10 μm thick for boronizing times of 2 h and 5 hours, respectively.
3. The hardness of boride layers changed in the range 1580 to 1602 HV, while the hardness of the core structure was in the range of 285–475 HV depending on the matrix microstructure.
4. Boro-tempering was more effective than traditional boronizing or austempering heat treatments. The sample boronized at 900 °C for 5 h and tempered for 1 h at 375 °C had an unnotched impact toughness of 79 J and a surface hardness of 1580 HV. Boro-tempering provided higher impact toughness than boronizing and also a higher surface hardness than austempering.

5. The fracture appearance of boro-tempered samples having an upper ausferritic core showed more dimples, characterizing the ductile fracture, when compared to lower ausferritic and pearlitic-ferritic core structure. However, the fracture surface through the boride layers had a columnar appearance. Impact test results revealed that the impact toughness of boronized and boro-tempered ductile cast iron is more related to the properties of the core than of the hard boride layer.

#### References

- [1] RUNDMAN, K. B.: ASM Handbook, 4, 1991, p. 682.
- [2] HARDING, R. A.—GILBERT, G. N. J.: *The British Foundryman*, 79, 1986, p. 489.
- [3] JANOWAK, J. F.—GUNDLACH, R. B.: *J. Heat Treating*, 1, 1985, p. 25.
- [4] VOIGT, R. C.—LOPER, C. R.: *J. Heat Treating*, 4, 1984, p. 291.
- [5] GUNDLACH, R. B.—JANOWAK, J. F.: *Metal Progress*, 128, 1985, p. 19.
- [6] BAYATI, H.—ELLIOTT, R.—LORIMER, G. W.: *Materials Science and Technology*, 11, 1995, p. 1007.
- [7] HARDING, R. A.: *Met. Mater.*, 2, 1986, p. 65.
- [8] JANOWAK, J. F.—MORTON, P. A.: *AFS Transactions*, 120, 1984, p. 489.
- [9] PUTATUNDA, S. K.: *Materials Science and Engineering*, A315, 2001, p. 70.
- [10] PALMER, K. B.: BCIRA Report 1722, January 1988.
- [11] PRADO, J. M.—PUJOL, A.—CULLELL, J.—TARTEIRA, J.: *Materials Science and Technology*, 11, 1995, p. 294.
- [12] ASLANTAŞ, K.—TAŞGETİREN, S.—YALÇIN, Y.: *Engineering Failure Analysis*, 11, 2004, p. 935.
- [13] ASLANTAŞ, K.—TAŞGETİREN, S.: *Wear*, 257, 2004, p. 1167.
- [14] HARDING, R. A.: *The Foundryman*, 86, 1993, p. 197.
- [15] BİNDAL, C.—ÜÇİŞİK, A. H.: *Surface and Coatings Technology*, 122, 1999, p. 208.
- [16] JAIN, V.—SUNDARARAJAN, G.: *Surface and Coatings Technology*, 149, 2002, p. 21.
- [17] ÖZBEK, İ.—AKBULUT, H.—ZEYİN, S.—BİNDAL, C.—ÜÇİŞİK, A. H.: *Surface and Coatings Technology*, 126, 2000, p. 166.
- [18] SINHA, A. K.: In: *ASM Int. Handbook. Vol. 4. The Materials International Society, Materials Park, OH, USA 1991*, p. 437.
- [19] STEWART, K.: *Ceram Ind.*, 146, 1996, p. 36.
- [20] SINGHAL, S. C.: *Thin Solid Films*, 45, 1977, p. 321.
- [21] BİNDAL, C.—ERDEMİR, A.: *Appl. Phys. Lett.*, 68, 1996, p. 923.
- [22] XU, C. H.—XI, J. K.—GAO, W.: *J Mater Process Technol*, 135, 1997, p. 94.
- [23] ÖZBEK, İ.—BİNDAL, C.: *Surface and Coatings Technology*, 154, 2002, p. 14.
- [24] MATUSCHKA, A. G.: *Boronizing. München, Carl Hanser Verlag 1987*, p. 1.
- [25] VOIGT, R. C.: *AFS Transactions*, 83, 1989, p. 253.